ML-reconstruction for TOF-PET with simultaneous estimation of the attenuation factors

Johan Nuyts [1], Ahmadreza Rezaei[1], Michel Defrise[2]

I. Introduction

In positron emission tomography (PET), attenuation correction is typically done based on information obtained from transmission tomography. Recently, it has been shown that stable maximum-likelihood reconstruction of both the attenuation and the activity from time-of-flight (TOF) PET emission data is possible [1], [2]. Mathematical analysis revealed that the TOF-PET data determine the attenuation correction factors uniquely except for a scale factor [3].

Here, we propose a maximum likelihood algorithm (called MLACF) that jointly estimates the image of the activity distribution and the sinogram with the attenuation factors. This method avoids the reconstruction of the attenuation image. If additive contributions (such as scatter and randoms) can be ignored, the algorithm even does not require storage of the attenuation correction factors. However, in contrast to [2], this algorithm does not impose the consistency of the attenuation sinogram, which may result in increased noise propagation. This paper presents the derivation of the algorithm, an (incomplete) theoretical analysis of the corresponding likelihood function, and first results on 2D and 3D simulations.

II. Methods

A. The MLACF reconstruction algorithm

The Poisson log-likelihood function is

$$L(y,a,\lambda) = \sum_i \sum_t \{-a_i p_{it} + y_{it} \ln(a_i p_{it} + s_{it})\} \quad (1)$$

$$p_{it} = \sum_j c_{ijt} \lambda_j \quad (2)$$

where i is the line-of-response (LOR) index, t is the TOF-index, a_i is the attenuation along LOR i, y_{it} is the measured (and therefore attenuated) TOF-PET sinogram, s_{it} is the known mean of the additive contribution (scatter and/or randoms). The attenuation-free TOF-PET "system matrix" [3] has elements c_{ijt} . The activity at voxel j is denoted as λ_j. We represent summations over the TOF-index by dropping that index: $s_i = \sum_t s_{it}$, $c_{ij} = \sum_t c_{ijt}$, $y_i = \sum_t y_{it}$ and $p_i = \sum_t p_{it}$.

We wish to estimate λ and a by maximizing (1). We propose an alternated optimisation: first a is updated keeping λ fixed, then λ is updated keeping a fixed. As shown below, a monotonic iterative algorithm that yields at least a local maximum of (1) is given by:

$$a_i^{k+1} = \frac{1}{p_i^k} \sum_t \frac{a_i^k y_{it} p_{it}^k}{a_i^k p_{it}^k + s_{it}} = a_i^k + \frac{a_i^k}{p_i^k} \left. \frac{\partial L(y,\lambda^k,a)}{\partial a_i} \right|_{a^k} \quad (3)$$

$$\lambda_j^{k+1} = \frac{\lambda_j^k}{\sum_i c_{ij} a_i^{k+1}} \sum_i a_i^{k+1} \sum_t c_{ijt} \frac{y_{it}}{a_i^{k+1} p_{it}^k + s_{it}} \quad (4)$$

where the superscript represents the iteration number. The second step is identical to standard MLEM, which is known to monotonically increase the likelihood. In the following, we show that the first step increases the likelihood as well.

B. Convergence

It is known that (4) increases the likelihood. Here we show that the same is true for (3). The maximizer a at fixed λ is a solution of

$$\frac{\partial L(y,\lambda,a)}{\partial a_i} = \sum_t \left\{ -p_{it} + y_{it} \frac{p_{it}}{a_i p_{it} + s_{it}} \right\} = 0 \quad (5)$$

If we consider only LORs for which $y_{it} > 0$ and $a_i p_{it} + s_{it} > 0$ (essentially LORs with activity), the second derivative is stricly negative and the maximizer a^* is unique and satisfies

$$1 = \frac{1}{p_i} \sum_t y_{it} \frac{p_{it}}{a_i^* p_{it} + s_{it}}. \quad (6)$$

The update step (3) has the following properties:
1) If $a_i^k < a_i^*$, then $a_i^k < a_i^{k+1} < a_i^*$.
Proof. If $a_i^k < a_i^*$, then $\partial L / \partial a_i > 0$, because L is a concave function with a unique maximum. Because the other factors in (3) are positive as well, it follows that $a_i^k < a_i^{k+1}$. If one replaces a_i^k with a_i^* in (3), the numerator increases with a larger factor than the denominator (since $s_{it} > 0$), and therefore $a_i^{k+1} < a_i^*$.
2) If $a_i^k > a_i^*$, then $a_i^k > a_i^{k+1} > a_i^*$. The proof is similar.
3) A fixed point of (3) is the maximizer of L. This follows immediately from (6).
4) The algorithm converges: $\lim_{k\to\infty} a^k = a^*$.
Proof. Combining (3) and (6) one obtains

$$a_i^{k+1} - a_i^* = \frac{a_i^k - a_i^*}{p_i} \sum_t \frac{y_{it} p_{it} s_{it}}{(a_i^k p_{it} + s_{it})(a_i^* p_{it} + s_{it})}. \quad (7)$$

Consider first the case where $a_i^0 < a_i^*$. Since $a_i^0 < a_i^k < a_i^*$ and since all quantities are non-negative,

$$\begin{aligned} |a_i^{k+1} - a_i^*| &\le \frac{|a_i^k - a_i^*|}{p_i} \sum_t \frac{y_{it} p_{it} s_{it}}{(a_i^0 p_{it} + s_{it})(a_i^* p_{it} + s_{it})} \\ &\le |a_i^k - a_i^*| c_i \frac{1}{p_i} \sum_t \frac{y_{it} p_{it}}{a_i^* p_{it} + s_{it}} \\ &= |a_i^k - a_i^*| c_i \ \le \ |a_i^0 - a_i^*| (c_i)^k, \quad (8) \end{aligned}$$

$$\text{with} \qquad c_i = \operatorname*{argmax}_{t, p_{it}>0} \frac{s_{it}}{a_i^0 p_{it} + s_{it}}, \quad (9)$$

where the restriction over the t range is due to the fact that terms with $p_{it} = 0$ do not contribute to the sum. With this restriction and $a_i^0 > 0$, one has $c_i < 1$ and $(c_i)^k \to 0$ and therefore $|a_i^k - a_i^*| \to 0$. The proof is similar for the case where $a_i^0 > a_i^*$. From this proof we expect the convergence rate to be of order (scatter fraction)^k.

C. Special case where scatter and randoms can be ignored

As suggested above, the convergence of the second step is extreme when the additive contribution s_{it} vanishes. Setting $s_{it} = 0$ in (4) and (3) results in the standard MLEM algorithm, except that in every iteration $k+1$ the attenuation values a_i^{k+1} are replaced with

$$a_i^{k+1} = \frac{y_i}{p_i^k}. \quad (10)$$

In this case, there is no need for separate storage of the attenuation sinogram, (10) can be directly inserted in (4).

[1] Nuclear Medicine, KU.Leuven, B-3000 Leuven, Belgium, [2] Nuclear Medicine, Vrije Universiteit Brussel, B-1090 Brussels, Belgium.

[3]The first and third dimensions correspond to the data dimensions, and could be combined to turn it into a real matrix

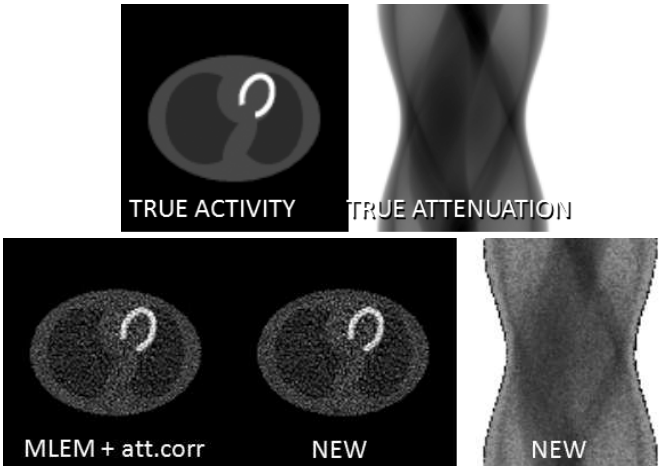

Fig. 1. The simulated true 2D activity distribution (top left) and the true attenuation correction factors (top right). The bottom row shows the OSEM reconstruction with exact attenuation correction, and the activity image and attenuation sinogram estimated with MLACF.

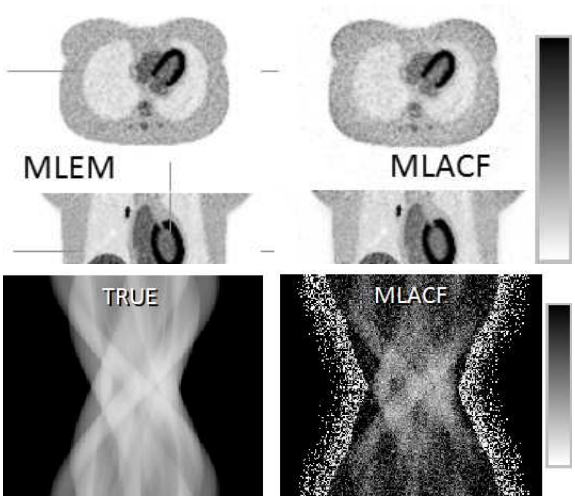

Fig. 2. Fully 3D simulation: the activity images reconstructed with MLEM and exact attenuation correction (top left), and with the new MLACF algorithm (top right). The bottom row shows the true attenuation factors (left) and the ones estimated by MLACF.

D. The curvature of the likelihood

The matrix of second derivatives of (1) is not negative semi-definite. However, semi-definiteness is a sufficient, but not a necessary condition to exclude local maxima. We currently have no results for the general case, here we show that there are no local maxima for the special case where the sinogram is consistent and where $\forall_{it} s_{it} = 0$. Using (10), one finds that in this special case the likelihood (1) reduces to

$$\tilde{L}(y, a, \lambda) = \sum_i \left(\sum_t y_{it} \ln(p_{it}) - y_i \ln(p_i) \right). \qquad (11)$$

Assume that $\hat{\lambda}$ is a solution that maximizes (11), satisfying $a_i \hat{p}_{it} = y_{it}$ (possible for a consistent sinogram). We consider an arbitrary image λ, and show that the gradient of the likelihood in λ always "points towards" this solution. More precisely, the projection of the gradient on the vector $\hat{\lambda} - \lambda$ is always positive. *Proof*: defining $\hat{p}_{it} = \sum_j c_{ijt} \hat{\lambda}_j$ we have

$$\begin{aligned} \sum_j \frac{\partial \tilde{L}}{\partial \lambda_j} (\hat{\lambda}_j - \lambda_j) &= \sum_i \left(\sum_t \frac{y_{it}}{p_{it}} \hat{p}_{it} - \frac{y_i}{p_i} \hat{p}_i \right) \\ &= \sum_i \frac{1}{a_i} \left(\sum_t \frac{y_{it}^2}{p_{it}} - \frac{y_i^2}{p_i} \right) \geq 0 \qquad (12) \end{aligned}$$

The last equality follows from the assumption. The inequality follows from the convexity of the square:

$$\sum_t \frac{y_{it}^2}{p_{it}} = p_i \sum_t \frac{p_{it}}{p_i} \left(\frac{y_{it}}{p_{it}} \right)^2 \geq p_i \left(\sum_t \frac{p_{it}}{p_i} \frac{y_{it}}{p_{it}} \right)^2 = \frac{y_i^2}{p_i}$$

III. Experiments

A. Simple 2D simulation

A noisy 2D attenuated TOF-PET sinogram was simulated. It had 120 radial bins of 3.33 mm, 120 angles over 180^o, a TOF resolution of 5 cm FWHM and 24 TOF bins. The scatter to primary ratio was 0.5. Images were reconstructed with standard OSEM using the exact attenuation correction factors, and with MLACF (120 $\times$ 120 pixels, pixel size of 3.33 mm). To ensure good convergence, 30 iterations with 20 subsets per iteration were applied for both algorithms. The true phantom and the obtained reconstructions are shown in figure 1. The noise was estimated as the difference between a reconstruction from noisy data (fig 1) and a noise free reconstruction. The correlation between this MLEM and MLACF noise, computed over all pixel values, was 0.91. This indicates that MLACF noise was very similar to that of MLEM, although MLACF had to estimate the attenuation factors as well, while MLEM used the exact attenuation factors.

B. 3D simulation

A part of the NCAT phantom was forward projected with a fully 3D TOF-PET projector, based on the specifications of the Siemens mCT scanner [4]. The sinograms had 200 radial bins of 4 mm, 168 angles over 180^o, 81 planes of 2 mm, 7 segments (i.e. 1 set of direct and 6 sets of oblique sinograms), 13 time bins of 312 ps, a TOF resolution of 580 ps FWHM, and a scatter to primary ratio of 0.5. Finite detector resolution was not modeled. The maximum pixel count in the TOF-PET sinogram was 52. Poisson noise was added to the data. The MLACF reconstruction was done with (3) and (4), where s_{it} was set to the exact noise-free scatter sinogram. For comparison, the same data set was also reconstructed with OSEM using the exact attenuation values. For OSEM 3 iterations with 21 subsets were applied, for MLACF we applied 4 iterations of 21 subsets, which seemed to give similar convergence by visual inspection. The results are shown in fig. 2.

IV. Discussion

The MLACF algorithm worked well on 2D and fully 3D TOF-PET simulations. In contrast to the MLAA-algorithm of [2], the MLACF does not impose consistency to the estimated attenuation factors, which may result in increased noise propagation. Although the first results indicate that noise propagation is not dramatic, we intend to make a detailed comparison between the MLAA and MLACF algorithms. Evaluation of the MLACF algorithm on real TOF-PET data is in progress.

References

[1] A. Salomon et al. "Simultaneous reconstruction of activity and attenuation for PET/MR", *IEEE Trans Med Imaging*, 2011; 30: 804-813.
[2] A. Rezaei et al. "Simultaneous reconstruction of activity and attenuation in time-of-flight PET", *IEEE Nucl Sci Symp Conf Record*, Valencia, Oct 2011, MIC8-7.
[3] M Defrise et al. "Time-of-flight PET data determine the attenuation sinogram up to a constant", *Phys Med Biol*, 2012, 57 (4), 885-899.
[4] M Conti. "Why is TOF PET reconstruction a more robust method in the presence of inconsistent data", *Phys Med Biol* 2011, 56: 155-168.